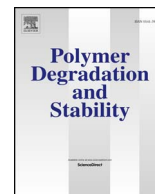




ELSEVIER

Contents lists available at ScienceDirect

Polymer Degradation and Stability

journal homepage: www.elsevier.com/locate/polydegstab

Fire retardant sol-gel coated polyurethane foam: Mechanism of action

S. Bellayer^{a,*}, M. Jimenez^a, B. Prieur^a, B. Dewailly^a, A. Ramgobin^a, J. Sarazin^a, B. Revel^b, G. Tricot^c, S. Bourbigot^a^a Univ. Lille, ENSCL, UMR 8207, UMET, Unité Matériaux et Transformation, F59652 Lille, France^b Univ. Lille, IMMCL, 59655, Villeneuve d'Ascq, France^c Univ. Lille, LASIR, UMR CNRS 8516, 59655, Villeneuve d'Ascq, France

ARTICLE INFO

Keywords:

Polyurethane foam

Flame retardant mechanism

Sol-gel

Coating

ABSTRACT

This paper investigates the flame retardant (FR) mechanism of action of a flexible PU foam, flame retarded with a sol-gel coating made of a mixture of tetraethoxysilane (TEOS), methyl triethoxysilane (MTES), 3-amino propyl triethoxysilane (APTES) and diethyl phosphite (DEP) in an ethanol/water solution. To build a mechanism of action, the coating as well as the residues obtained after fire testing were analyzed using solid state nuclear magnetic resonance (NMR), rheology, thermogravimetric analyses coupled with infrared detection (TGA-FTIR), microcalorimetry of combustion (MCC), smoke box and Pyrolysis Gas chromatography coupled with mass spectrometry (Py-GCMS). The coating shows an intumescent behavior upon burning exhibiting significant expansion and bubbling. The expansion occurs in two steps: a first step around 190 °C, related to the release of ethanol, and a second one around 380 °C, related to the release of non-degraded DEP, ammonia and propylene during degradation of the PU matrix. The flame retardant effect occurs (i) in the condensed phase by intumescence, which yields a thermal insulating layer made of a SiO₂ and Si-O-P network mixed with orthophosphate at the surface of the PU foam, but also (ii) in the gas phase by the release of non-degraded DEP, which acts as free radical scavenger. The coating allows the protection of the underlying PU foam during burning as well as the reduction of the amount of smoke released.

1. Introduction

Flexible polyurethane foam is a chemically complex polymeric product having a broad range of load-bearing capability and resiliency, offering comfort as a cushioning material for furniture, bedding, carpet underlay and automotive interiors. It also offers protective shock absorption performance for use in packaging and automotive applications.

The flame retardants used to protect PU foams are still mainly halogenated and some are associated with a wide range of adverse effects in animal and human health, including endocrine disruption, immunotoxicity, reproductive toxicity, effects on fetal/child development, thyroid and neurologic function, and cancer [1,2]. Some flame retardants, such as polybrominateddiphenyl ethers (PBDEs), have been banned or voluntarily phased out by manufacturers because of their environmental persistence and toxicity [3], and were replaced by other organohalogens. However, most fire deaths and fire injuries result from inhaling carbon monoxide, irritant gases, and soot; it is also reported that the incorporation of organohalogens can increase the yield of these toxic by-products during combustion [4].

Despite restrictions on further production of halogen FR additives in

some countries, consumer products previously treated with banned retardants are still in use. Thus, the tendency is to replace first generation products having high-embodied energy in favor of eco-friendlier products, without losing their structural and functional properties such as flexibility and resilience. However, it is difficult to make fire retardant foams because of their manufacturing process, which is usually incompatible with the flame retardant additives commonly used (powder in particular). Indeed, the flame retardant additives are mostly incompatible with the foaming process and have negative effects on the physical properties and/or aging behavior of the foam [5–7].

The new trend is now to avoid the issues encountered by the incorporation of FR additives during the manufacturing process of foams by treating the entire final product with innovative surface treatments (layer by layer [8–11], plasma [12] or sol-gel [13] treatments).

A sol-gel process, recently published by our group [13], has been reported to efficiently fire retard PU flexible foams: PU foams were impregnated with a proper ratio of tetraethoxysilane (TEOS) and methyl triethoxysilane (MTES) with (3-amino propyl triethoxysilane) (APTES) and diethyl phosphite (DEP) in an ethanol/water solution. It led to a self-extinguishing PU foam when exposed to flame for 10 or

* Corresponding author. Ecole Nationale Supérieure de Chimie de Lille (ENSCL), Cité Scientifique Bât C7a, Av Mendeleiev, BP 90108–59652 Villeneuve d'Ascq Cedex, France.
E-mail address: severine.bellayer@ensc-lille.fr (S. Bellayer).

60 s under UL-94 conditions. Moreover, a mass loss calorimeter test was also carried out at 50 kW/m² and a 60% decrease of the peak Heat Release Rate (HRR) was observed, as well as a micro intumescent phenomenon. However, the flame retardant mechanism of action was not elucidated.

Thus in this paper, both the coating alone and the coated PU foam have been studied using solid state magic angle spinning nuclear magnetic resonance (MAS-NMR), rheology, thermogravimetric analyses coupled with infrared detection (TGA-FTIR), microcalorimetry (MCC), smoke box and Pyrolysis Gas chromatography coupled with mass spectrometry (Py-GCMS), in order to build a FR mechanism of action and understand the phenomena occurring both in the condensed and gas phases during combustion.

2. Experimental part

2.1. Raw materials

Samples were cut from open-cell flexible molded polyurethane foams provided by Saira Seats, France and were used as received without further cleaning. The Saira Seats foams (density of 50–80 kg/m³) are composed of more than 98 wt% polyurethane and less than 2 wt % bis-chloromethylenebis (bis- 2-chloroethyl)phosphate (Amgard V6, CAS no. 38051-10-4). They are obtained by (i) polymerization of a polyol on an isocyanate and (ii) release of carbon dioxide resulting from the polycondensation of an isocyanate on a water molecule. Both reactions occur simultaneously, and the components are added in stoichiometric amounts, in order to guarantee the total polymerization and neutrality of each reactive function (hydroxyl, amine, isocyanate), resulting in an inert polymer without any free monomer.

Chemical products, i.e., tetraethoxysilicate (TEOS, 98% purity), methyltriethoxysilicate (MTES, 95% purity), 3-amino propyl triethoxysilane (APTES, 97% purity), diethyl phosphite (DEP, 99% purity) and Tin II 2 ethylhexanoate (TEH, 92.5–100% purity) were purchased from Sigma Aldrich, France.

2.2. Sol-gel process

The optimized FR sol-gel formulation used was already investigated elsewhere [13]. 10.8 ml ethanol with 5.8 ml TEOS and 1.44 ml MTES were mixed for 10 min in a 250 ml beaker. Then, 6.5 ml of DEP and 12 mL of APTES were added to the mixture and stirred for 5 min before the addition of 216 ml of deionized water (Sol/4APTES/2DEP). After 5 min of stirring, 0.3 ml of the TEH catalyst was added.

For comparison, a coating containing only TEOS and MTES with TEH in the water/ethanol mixture (Sol) was also formulated in the same volume.

When analyzed by itself without PU foam, the solution was poured into an alumina plate and left for 1 h at 70 °C in a convection air oven and for 2 days at room temperature before characterization.

When coated, PU foams were immersed in the solution and pressed 4 times for solution absorption. The foams were finally left to drip-dry for 1 h at 70 °C in a convection air oven and 2 days at room temperature before characterization.

2.3. Solid state NMR

²⁹Si and ³¹P MAS-NMR measurements were performed on a 9.4 T Bruker Avance I spectrometer at 79.4 and 161.9 MHz, respectively. The ²⁹Si MAS-NMR experiments were conducted at a spinning frequency (ν_{rot}) of 5 kHz with a HX-7mm probehead using a 5 μ s pulse length ($\pi/2$), a recycle delay (rd) of 120 s and 192 transients. The ³¹P MAS-NMR spectra were recorded under ¹H decoupling condition at $\nu_{\text{rot}} = 10$ kHz on a HX-4mm probehead. The acquisitions were performed with a 4 μ s pulse length ($\pi/2$), a rd of 60 s and 16–32 transients. The ²⁹Si and ³¹P chemical shifts were referred to TMS and H₃PO₄ as 0 ppm. The ³¹P/²⁹Si

spatial proximity was investigated by correlation NMR technique in order to highlight the presence of phosphosilicate moieties. A filtered 1D ³¹P NMR spectrum was edited with the ³¹P (²⁹Si) D-HMQC NMR sequence [14] to reveal the P atoms involved in P/Si close proximity. The correlation experiment was conducted on a HXY-4mm probehead at $\nu_{\text{rot}} = 10$ kHz with ³¹P and ²⁹Si $\pi/2$ pulse lengths of 4.25 and 5 μ s, a rd of 60 s, 8192 transients and a SR4₁² recoupling scheme applied on the ²⁹Si channel during 4 ms. It is noteworthy that all the acquisition parameters were first optimized on a 100% enriched ²⁹Si crystalline SiP₂O₇ sample.

2.4. Rheological test

Rheological measurements were carried out using a Rheometric Scientific ARES 20 A thermal scanning rheometer in a parallel plate configuration. Samples were positioned between the two plates. A constant normal force of 10 g (200 Pa) was systematically applied in order to obtain good adhesion between samples and plates. The operating conditions were: a strain value of 1% and a frequency of 1 rad/s. The relative expansion of the samples as well as the complex viscosity values were recovered over the complete temperature range (50–500 °C) with a heating rate of 10 °C/min.

2.5. Microcalorimeter (MCC)

A microcalorimeter, also known as a Combustion flow calorimeter (MCC) (Fire Testing Technology, UK) was used to determine on a milligram scale the flammability characteristics of PU foams, following ASTM D7309. PCFC is a useful instrument to determine the fuel content of the decomposing volatile products and can also offer valuable insight into the action mechanism of the FRs. In the MCC technique, the gases released during the pyrolysis are evacuated into an oven at 900 °C containing a 80/20 N₂/O₂ mixture. In these conditions, total combustion of these gases takes place. The MCC calculates the HRR by measuring the oxygen consumption. Each sample (approximately 7 mg) was exposed to a heating rate of 60 °C/min from 150 to 750 °C in the pyrolysis zone. Through MCC, the peak of heat release rate (pHRR) was measured. The results obtained were corrected after conducting a TGA under nitrogen atmosphere of each sample. The conditions of the TGA were the same as that of the PCFC (60 °C/min to 750 °C, under nitrogen atmosphere). The residual mass at a given temperature allowed the calculation of the specific heat release rate at any given temperature.

2.6. TGA FTIR

Gases released during the degradation of the virgin foam and of the coated foams were analyzed using a TGA apparatus (TGA Q5000, TA Instrument) connected to a Fourier transformed infrared (FTIR) spectrometer (ThermoScientific) Nicolet iS10. The IR spectra were recorded between 400 cm⁻¹ and 4000 cm⁻¹ (spectra recorded every 5 s). For each experiment, samples of 10 mg of material were positioned in alumina open pans. All the analyses were carried out in nitrogen flow, Air Liquide grade (100 mL min⁻¹) from 30 °C up to 800 °C with a 10 °C/min temperature ramp.

2.7. Mass loss cone

A Fire Testing Technology (FTT) Mass Loss Calorimeter (MLC) was used to perform experiments on samples following the procedure ASTM E 906. The equipment is identical to that used in oxygen consumption cone calorimetry (ISO 5660), except that a thermopile in the chimney is used to obtain HRR rather than employing the oxygen consumption principle. Coating samples (10 cm × 10 cm × 1 mm) were tested in horizontal orientation. Samples were deposited in aluminum foil leaving the upper surface exposed to the heater (external heat flux = 50 kW/m²) and placed on a ceramic backing board at a distance

of 35 mm from cone base.

2.8. Pyrolyser GCMS

Pyrolysis-GC/MS is an extremely sensitive tool used to determine the nature of gases evolved during the thermal decomposition of a material. The pyrolysis-GC/MS measuring system was provided by Shimadzu. A micro-furnace pyrolyzer (Frontier Lab PY-2020iD), a gas chromatograph equipped with a capillary column and a quadrupole mass spectrometer equipped with an Electron-Impact (EI) ionization source (Shimadzu GC/MS QP2010 SE) are directly connected in series. About 0.2 mg of the sample is added in a stainless steel sample cup. The latter is first placed at the upper position of the pyrolyzer, and then introduced into the center of the furnace (inside a quartz tube vial) under a helium gas flow. In the pyrolyzer furnace, the temperature was initially set at 35 °C and then raised to a defined temperature with a selected heating rate. The temperature of the GC injection port and of the interface between the pyrolyzer were respectively set at 280 °C and 320 °C. A fused silica capillary column (30 mm × 0.25 mm × 0.25 mm thickness) was used and the linear velocity of helium as a carrier gas was 40 cm/s. The GC column temperature was maintained at 35 °C during the whole temperature ramp of samples in the pyrolyzer and then programmed up to 300 °C at a rate of 5 °C/min, followed by an isotherm of at least 10 min at 300 °C. The studied PU foams or coatings by themselves were submitted to a ramp of 10 °C/min from 35 to 800 °C in an inert atmosphere (He) in the pyrolyzer, while volatile compounds were observed, and then the heavier compounds were desorbed. Electron-impact spectra were recorded at 85 eV with a mass scan rate of 2 scans per s. Pyrograms and mass spectra were treated using a GC/MS post run analysis program (Shimadzu). The NIST and FSearch mass spectral databases were used for the identification of products.

2.9. Smoke box experiment

Smoke box experiments (ISO 5660-1) were carried out at 25 kW/m² on 10 cm × 10 cm × 2 cm samples at the CREPIM test center following the standard EN45545-2+41 to measure the release rate of CO₂ and CO during burning.

3. Results and discussion

It has been previously reported that when PU foam is coated with Sol/4APTES/2DEP formulation [13], a micro intumescent char forms when a flame is applied which induces self-extinguishing behavior at UL94 test and a 60% decrease of the HRR peak under mass loss cone conditions. In order to try to evidence this phenomenon, the Sol/8APTES/4DEP coating was first investigated without the PU foam substrate to characterize the intrinsic intumescent property of the coating.

- Study of the mechanism of action of the FR coating Sol/4APTES/2DEP

First, thermal rheological experiments were carried out on the coating alone. Indeed, in literature, it has been found that recording the gap between the two parallel plates of the device during the whole heating ramp of the rheological experiment can give a good indication of the height of the intumescent phenomenon versus temperature [15,16]. Both the relative expansion of the sample and the complex viscosity were registered simultaneously. Fig. 1 shows the complex viscosity of the coating and the expansion rate of the sample versus temperature. It is obvious that the coating expands during temperature increase, confirming its intumescent properties. Two expansion steps are noticeable. The first starts around 180 °C (300% expansion), followed by a plateau between 250 and 320 °C and the second starts around 320 °C to reach a 450% expansion at 500 °C. A decrease of the

complex viscosity is noticeable before each expansion whereas an increase is observed during expansion. At 190 °C, a white and foamy residue is produced, meaning that the organic part of the sol-gel is not degraded yet and at 380 °C a brittle black foam-like residue is observed (Fig. 1a). The two steps of swelling are well correlated with the two main steps of degradation visible on the TG degradation curve of the coating (Fig. 1b).

Thus, the Sol/4APTES/2DEP coating is intrinsically intumescent and does not need the substrate to expand during burning.

Chemical characterization of the non-degraded coating and of the degraded residue were performed in order to better understand the chemical changes occurring in the condense phase during burning. The residue analyzed by solid state NMR is a mass loss cone char obtained after the exposition of a 1 mm thick Sol/4APTES/2DEP coating deposited on aluminum foil to a 50 kW/m² heat flux. During the mass loss experiment, the coating swells from 1 mm up to 30 mm and a foam-like structure is obtained, containing a network of bubbles with different sizes (Fig. 2). The top layer of the char is black and the bottom layer is white, showing the temperature gradient occurring in the residue during the mass loss cone experiment.

For solid-state NMR experiments, only the black top layer directly exposed to the 50 kW/m² heat flux is recovered. Both samples, non-degraded coating and degraded residue, were first analyzed by solid-state NMR spectroscopy to analyze their chemical composition and to characterize the reticulation state of the silicon network. The ²⁹Si NMR spectrum of the Sol coating (i.e. without FR monomers) (Fig. 3a) was compared to the one of the Sol/4APTES/2DEP coating (Fig. 3b). In the silica network of the Sol coating, more Q3 and Q4 structures than T0, T2 and T3 ones were identified [17,18]. In the case of the Sol/4APTES/2DEP the structure is not as cross-linked as the Sol: indeed, more T3 structures than Q3 and Q4 ones were identified. This result is consistent with the fact that APTES is less reactive than TEOS and MTES because of the nitrogen group, thus preventing a high crosslinking rate. After burning, since all organic groups have been decomposed at high temperature, a great increase in crosslinking rate is noticed: the structure of the residue shows only Q4 structures (SiO₂ species).

³¹P solid NMR was also performed on the Sol/4APTES/2DEP before and after burning (Fig. 4a and b). Before burning, only the peak characteristic of DEP structure appears at 4 ppm. After burning, several peaks appear. The peak at 0 ppm is attributed to Q0 species (such as phosphoric acid and/or orthophosphates), the peaks at -5 ppm and -11 ppm to pyrophosphate species [19–21]. The broad peak between -30 ppm and -50 ppm is attributed to silicophosphate structures from a previous publication [22]. This attribution has been confirmed by the editing of a filtered ³¹P NMR spectrum (Fig. 4c) that only shows the ³¹P signals involved in significant ³¹P/²⁹Si dipolar interaction, i.e. phosphate species involved in phosphosilicate structures.

DEP thus mainly turns into phosphoric acid during degradation, which makes it one crucial ingredient of the intumescent system, i.e. the acid source.

To conclude on the ²⁹Si and ³¹P NMR results, the degradation of the coating leads to a residue of a highly cross-linked SiO₂ network containing orthophosphate species. Since it is well known that a SiO₂ network acts as a thermal insulator [23] and phosphoric acid as a char promoter [24], it is thus confirmed that the Sol/4APTES/2DEP coating acts in the condensed phase by creating a solid insulative cross-linked network, which should protect the underlying PU foam substrate from fire.

In order to study the gas phase, the released gases were first analyzed using a pyrolyser GC-MS. Fig. 5 shows the spectrum of the emitted gases of the Sol/4APTES/2DEP after pyrolysis. In this case, three noticeable areas were detected (brackets) and the emitted gases were attributed thanks to their mass spectra. Ethanol (between 35 and 45 min) and propylene and ammonia (between 65 and 85 min), which can be by-products of APTES, can be identified on the spectrum. Non-degraded DEP was also identified between 55 and 105 min. It was released

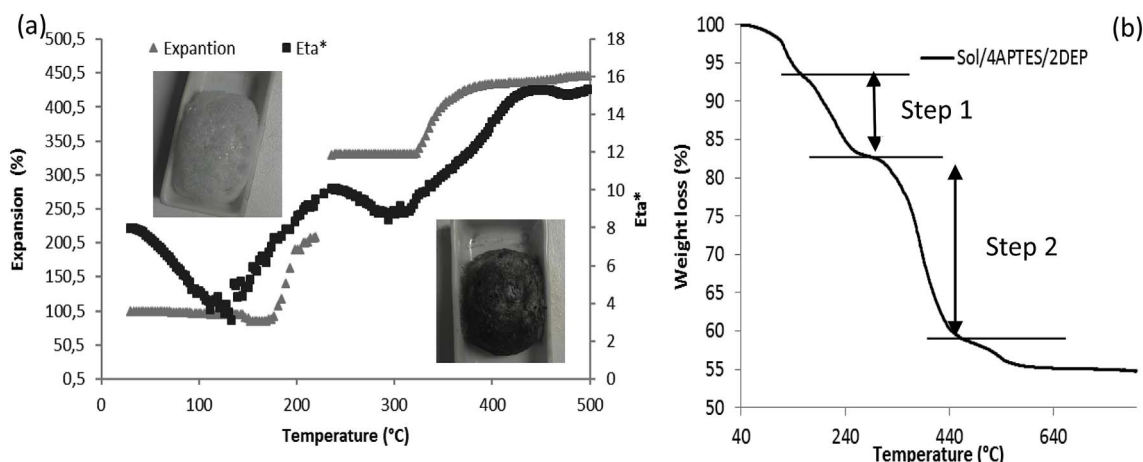


Fig. 1. Viscosity and relative expansion of Sol/4APTES/2DEP (no PU substrate) measured during the rheological test with the picture of the residues obtained at 190 °C and 380 °C (a) and the corresponding TGA curve (b).



Fig. 2. Picture of a cross section of the mass loss cone char obtained after exposition to a 50 kW/m² heat flux of a 1 mm thick Sol/4APTES/2DEP coating deposited on aluminum foil.

directly in the gas phase without degradation.

Since the emitted gases were identified, TGA-FTIR analyses were carried out on the Sol/4APTES/2DEP (still without PU foam substrate) to find out at what temperature each gas is released and to identify the gases responsible for the expansion of the coating during burning. Fig. 6 shows the FTIR spectra of the emitted gases after 19 and 36 min in the TGA oven, which respectively correspond to 220 °C and 390 °C, i.e. to the two characteristic temperatures of the expansion steps observed during the rheometry test.

At around 190 °C (19 min) and for several minutes the FTIR spectrum shows peaks at 900 cm⁻¹, 1050 cm⁻¹, 1250 cm⁻¹, 1400 cm⁻¹ and 3680 cm⁻¹ and a broad peak between 2900 and 3000 cm⁻¹. Those peaks fit the spectrum of pure ethanol in the gas phase [25]. At around

390 °C (36 min) and also for several minutes, the FTIR spectrum shows numerous peaks, which mainly correspond to three different compounds. The broad peaks at 1250 cm⁻¹ (P=O), 1050 cm⁻¹ (P-O-ethyl), 947 cm⁻¹ (P-O), 2981 cm⁻¹ (CH₃) are characteristic of the DEP compound [26,27]. The numerous thin peaks around 3320 cm⁻¹ and those between 800 cm⁻¹ and 1200 cm⁻¹ are characteristic of the release of ammonia gas (NH₃). The peaks lying between 3500 and 3800 cm⁻¹ and 1400 and 1700 cm⁻¹ are attributed to the release of water (H₂O) [28]. Finally, the shoulder around 3050 cm⁻¹ is attributed to the release of propylene (=CH₂). The other vibration bands of propylene are hidden by the vibration of the other compounds.

Thus, TGA FTIR confirms that non-degraded DEP is released in the gas phase. Therefore, the coating can possibly also have a FR effect in the gas phase since DEP can act as flame retardant in the gas phase through PO mechanism (radical scavengers) [24,29].

To summarize, in addition to building a Si-O-Si network during burning, the Sol/4APTES/2DEP coating is intrinsically intumescent; the swelling occurs in two different steps, the first one due to the release of ethanol around 220 °C and the second one due to the release of DEP, ammonia and propylene around 390 °C. As non-degraded DEP is released during burning, DEP can also act as a flame retardant in the gas phase. This FR behavior of the coating was then compared to the behavior of the same system but with PU foam.

- FR mechanism of action of the coating in the presence of PU foam

NMR experiments were carried out on the residue obtained after the mass loss cone experiment at 50 kW/m² (experiment not shown) in order to check if the PU foam interfered with the condensed phase

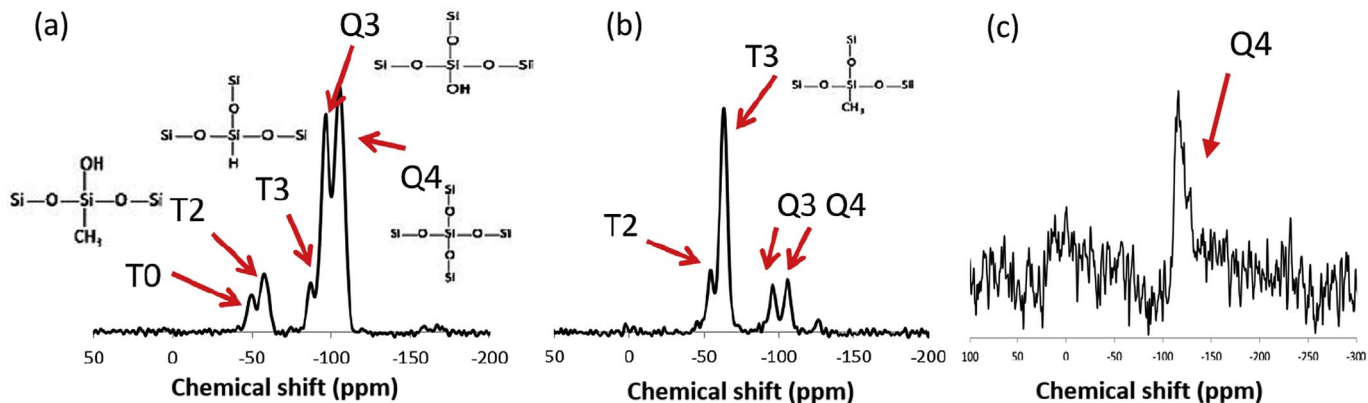


Fig. 3. ²⁹Si NMR spectra of Sol (a), Sol/4APTES/2DEP (b) and of Sol/4APTES/2DEP residue obtained after the mass loss cone (c).

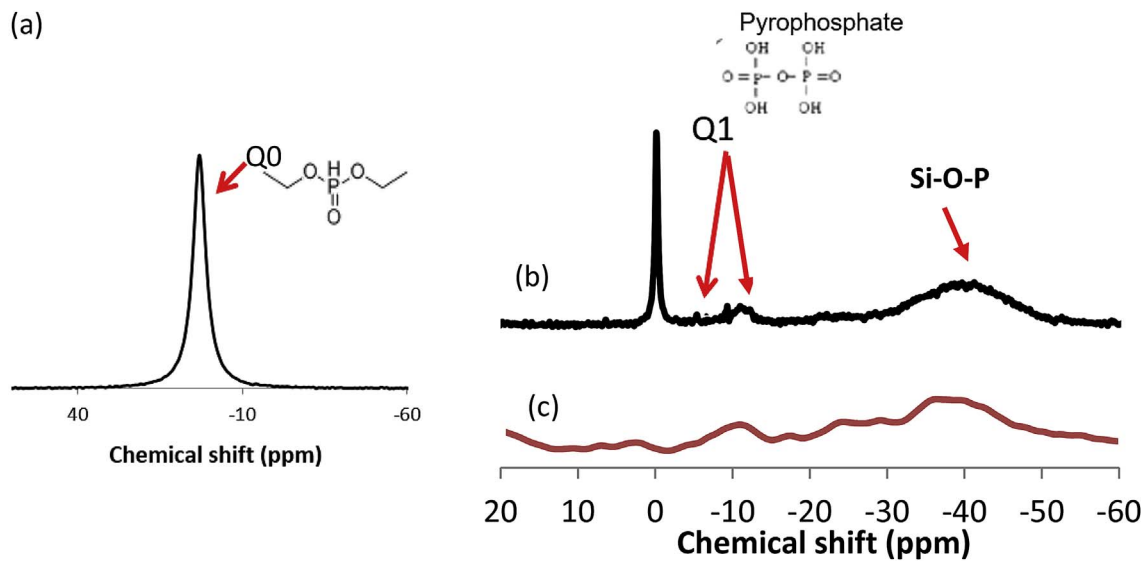


Fig. 4. ^{31}P NMR spectra of Sol/4APTES/2DEP coating before burning (a) and of the Sol/4APTES/2DEP coating residue obtained after the mass loss cone (b). Filtered ^{31}P NMR spectra obtained by the ^{31}P (^{29}Si)D-HMQC NMR sequence (c).

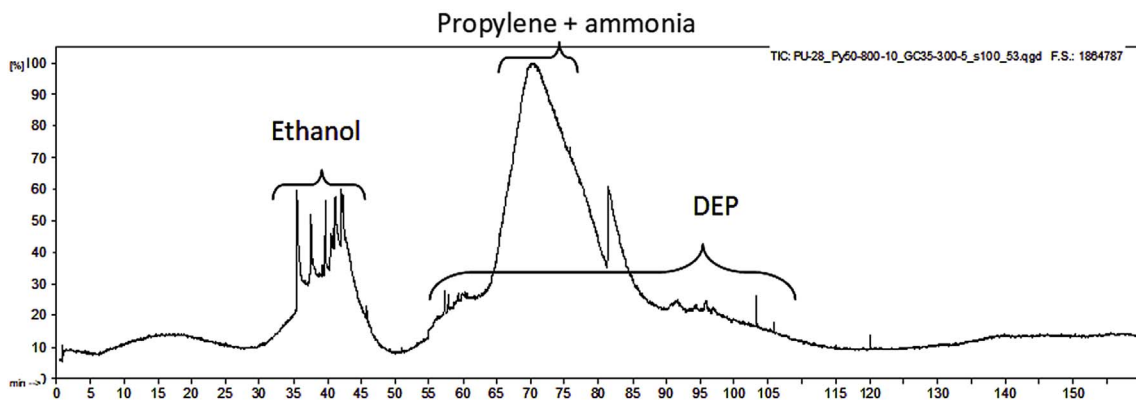


Fig. 5. Py-GCMS spectrum of Sol/4APTES/2DEP (without PU foam) and attribution of the main peaks.

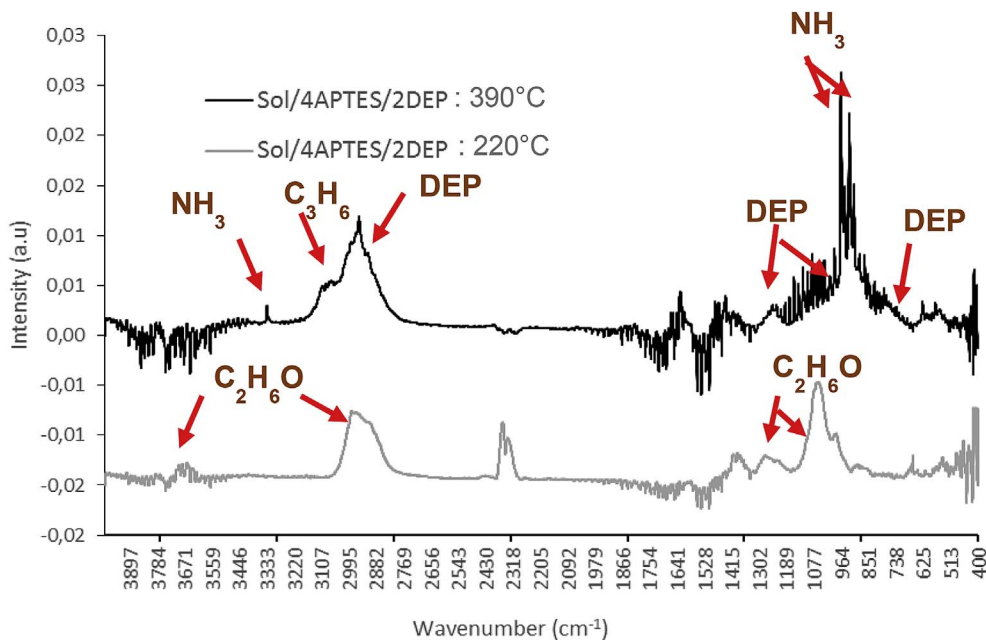


Fig. 6. TGA-FTIR spectra at 220 °C and 390 °C of Sol/4APTES/2DEP alone without PU foam.

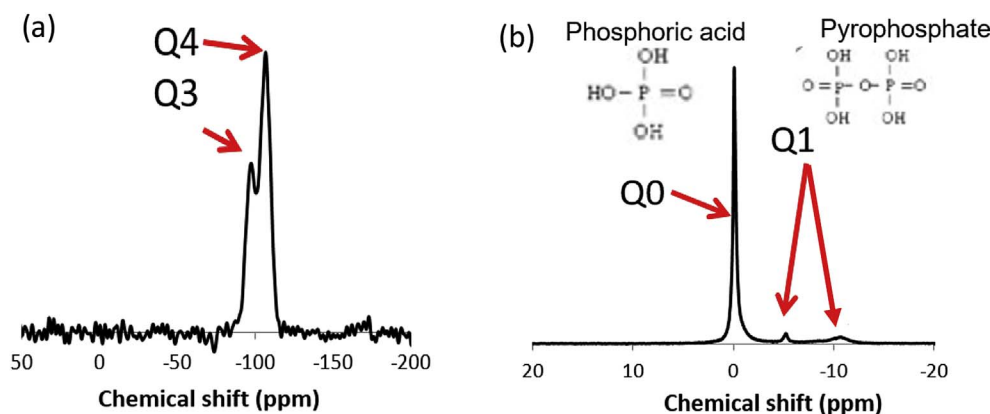


Fig. 7. ²⁹Si (a) and ³¹P (b) NMR spectra of Sol/4APTES/2DEP treated PU foam residue obtained after the mass loss cone.

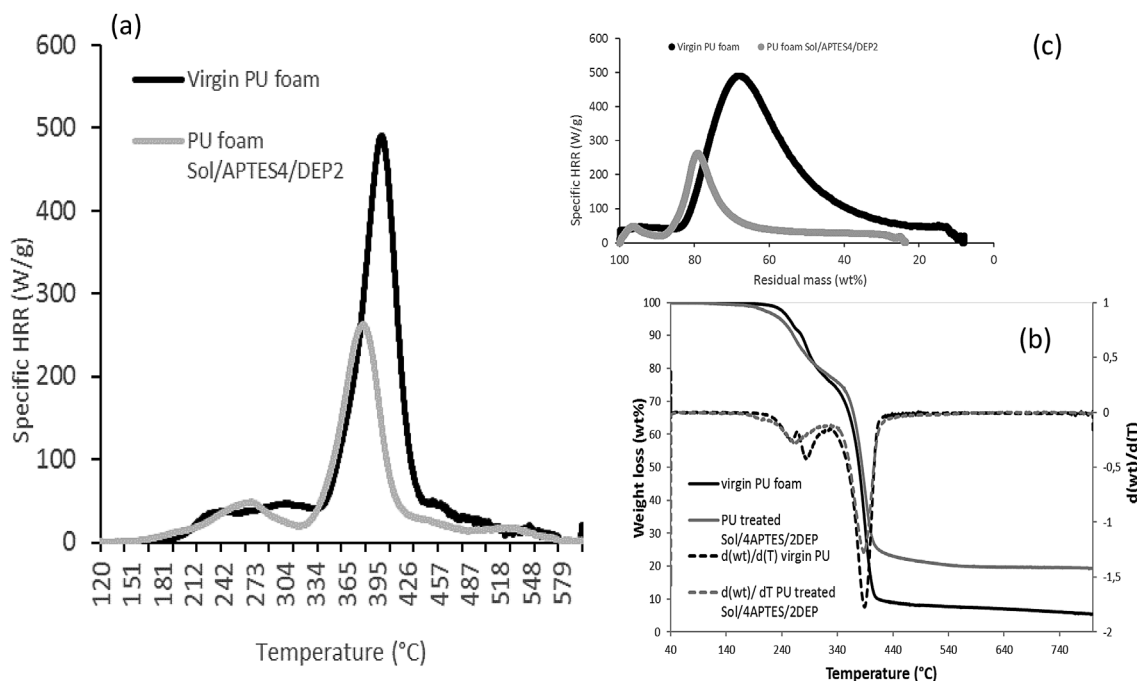


Fig. 8. Corrected MCC specific HRR curves of virgin PU foam and Sol/4APTES/2DEP treated PU foam (a), the corresponding TGA and DTG curves (b) and HRR versus residual mass calculated curves (c).

Table 1
 pHHR values obtained by mass loss cone and MCC experiments and the corresponding calculated percentage of physical and chemical mechanism occurring during burning.

	Mass loss cone pHHR [13] (kW/m ²)	Decrease (%)	MCC pHRR (W/g)	Decrease (%)	Chemical mechanism (%)	Physical mechanism (%)
Virgin PU foam	400	/	500	/	/	/
PU foam Sol/APTES4/DEP2	170	57,5	280	44	76%	24%

effect of the coating. The ²⁹Si and ³¹P NMR spectra (Fig. 7a and b) were compared to those obtained without PU foam (Figs. 3c and 4b). It can be noticed in Fig. 6a that when the PU foam is present, the structure of the residue is composed of a mixture of Q3 and Q4 species and not only Q4 as in the coating residue. The PU foam prevents the appearance of a well reticulated SiO₂ structure; however, a highly cross-linked network is still formed. In the ³¹P spectra, the only difference with spectra obtained without PU foam is the disappearance of the broad peak between -30 and -50 ppm, attributed to silicophosphate structures. The presence of PU foam prevents the formation of the Si-O-P structure.

It has been previously shown that the coating also has a FR mechanism of action in the gas phase. To verify that the coating does not lose this ability when applied on PU foam, MCC experiments were carried out on both virgin PU foam and PU foam coated with Sol/

4APTES/2DEP. Fig. 8a reports the MCC HRR graphs of virgin and coated PU foams. Two HRR peaks are observed at 276 °C and 400 °C for raw PU foam. The combustion of flexible polyurethane foams is, indeed, known to be a process with two main steps [12], as also reported by TGA (Fig. 8b). The first step (276 °C) corresponds with the melting and degradation of the foam into a tar and the second step (400 °C) with the combustion of the tar previously produced. These two degradation steps lead to two distinct HRR peaks. The coated PU foam also degrades in two steps (Fig. 8b), and both HRR peaks are shifted to lower temperatures (Fig. 8a) compared to raw PU (to 272 °C and 387 °C, respectively). Moreover, a reduction of the second HRR peak of about 45% was observed for the coated PU foam (200W/g) compared to raw PU foam (380 W/g).

These microcalorimeter results can be explained by two hypotheses:

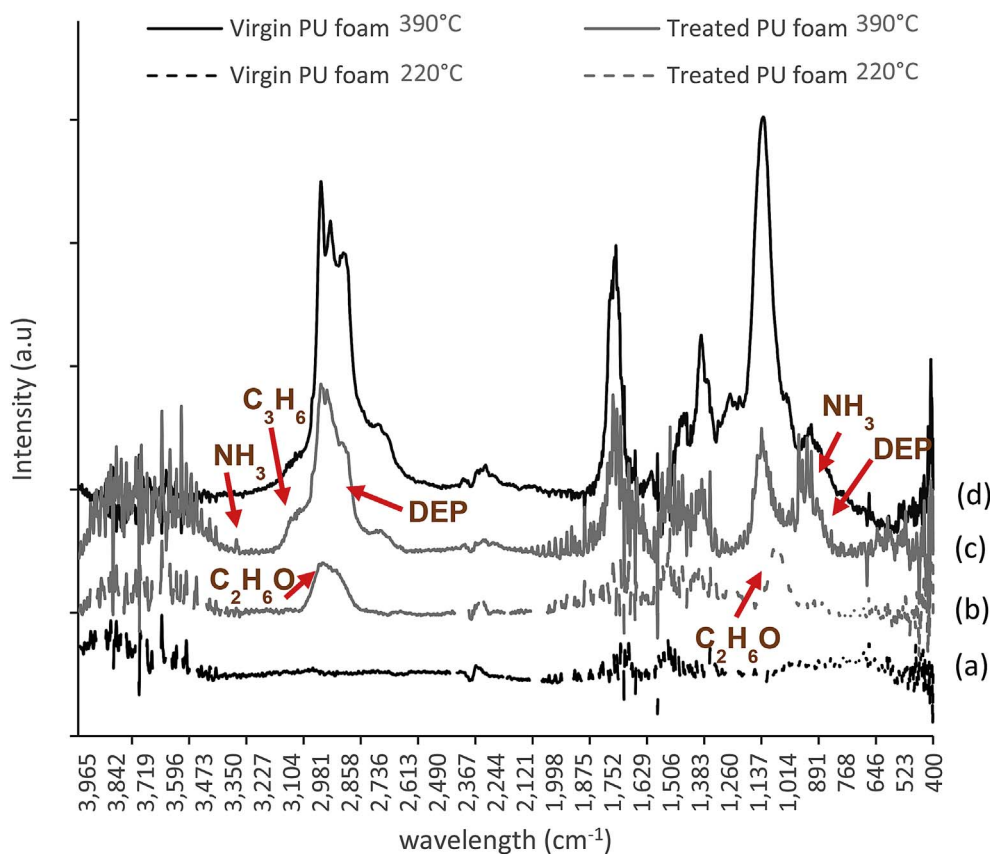


Fig. 9. TGA-FTIR spectra at 220 °C and 390 °C of virgin PU foam (a and d) and PU foam treated with Sol/4APTES/2DEP (b and c).

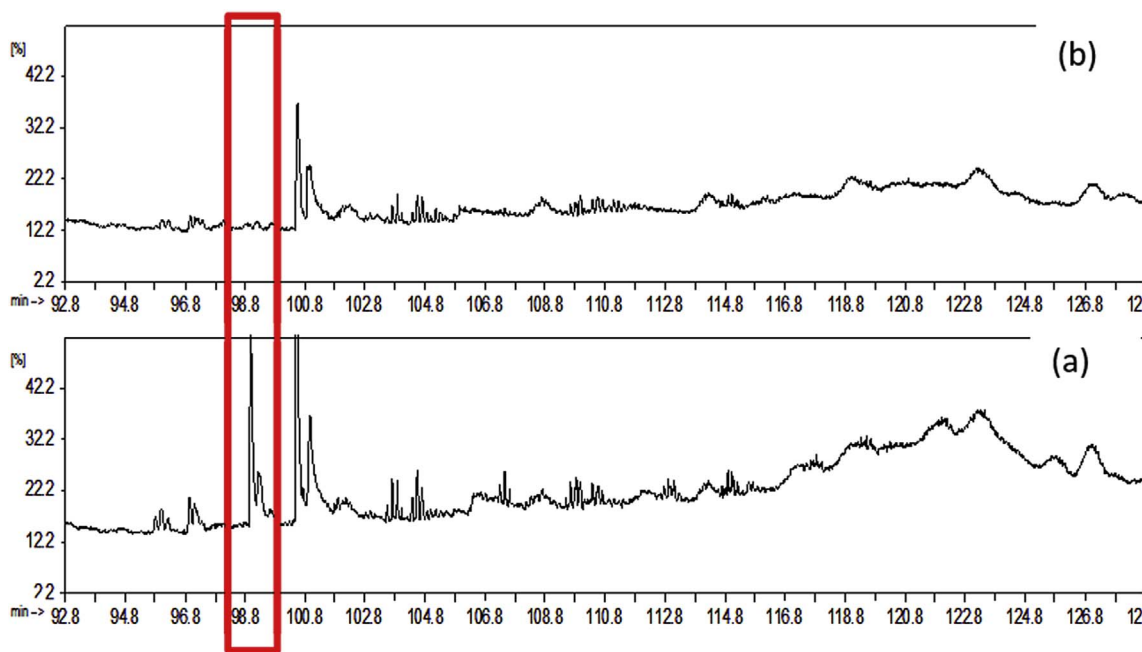


Fig. 10. Py-GCMS pyrograms of virgin PU (a) and PU treated with Sol/4APTES/2DEP (b).

(i) the sol-gel coating partly flame retards the foam by a gas phase mechanism, or (ii) the FR mechanism is a condensed phase mechanism with the coated PU foam releasing a smaller amount of gases than raw PU foam. To confirm or refute these hypotheses, MCC curves were compared to TGA and related DTG curves as well as mass loss cone curves obtained previously. The second combustion step observed by MCC at around 400 °C fits well with the second main degradation step observed by TGA. The degradation of the coated foam leads to a 22 wt.-%

residue at 800 °C, compared to no residue for the raw PU foam (Fig. 8b). The theoretical residue (i.e. if there was no interaction between the coating and the foam) can be calculated from the two TGA measurements of the coating by itself and of the virgin foam, considering an add-on of 28 wt.-%, already published previously [13]. The theoretical calculated residue was found to be 15 wt.-%. Thus, there is a 7% weight gain between the theoretical calculated residue and the practical experimental result. It has been noticed by solid state NMR

Table 2
 CO₂ and CO release rate (mg/m³) at 25 kW/m² under smoke box conditions.

	4 min Virgin PU foam	4 min Coated PU foam	8 min Virgin PU foam	8 min Coated PU foam
CO ₂ release (mg/m ³)	15174, 1	12547, 7 (-20%)	18637, 4	16769, 2 (-10%)
CO release (mg/m ³)	228, 1	166, 6 (-35%)	320, 8	235, 8 (-35%)

and FTIR that DEP partially degrades into phosphoric acid, and phosphoric acid is known to promote charring by modifying the degradation pathway of the polymer. As a conclusion, one part of the HRR decrease observed with MCC experiments can be explained by a condensed phase mechanism, the degradation gases being partially trapped to create a thermal insulative residue (7% weight gain). In order to verify that part of the decrease of the HRR peak is also due to a gas phase mechanism, the MCC results were correlated with the TGA curves i.e., the specific heat release rate as a function of residual mass. This allowed the observation of the evolution of the mass of the sample as well as the degree of decomposition at which there is a notable release of combustibles [30]. This led to a representation of the amount of heat released with respect to the remaining mass of the samples (Fig. 8c). It can be noticed that both virgin PU foam and sol-gel treated PU HRR values start to increase at the same weight loss (75–80 wt%), which correlates well with the start of the second degradation step observed with TGA. However, the increase of HRR values stops very quickly (82% weight loss, 380 °C) for the sol-gel treated PU foam compared to virgin PU foam (65% wt loss, 395 °C). Thus, the HRR values of the sol-gel treated PU foam start to decrease at the same temperature as the one of the release of ammonia and DEP in the gas phase, which demonstrates that the FR mechanism can also partially occur in the gas phase.

It has also been seen in the literature [31,32] that it is possible to determine by which pathway (physical or chemical) fire protection mainly occurs by comparing the decrease of pHRR obtained by MCC and by cone calorimeter tests. This can be done because MCC values corrected as a function of residual mass takes mainly into account mechanisms occurring by chemical pathways, whereas the cone calorimeter results are mostly affected by both, chemical and physical mode of action. Table 1 presents the pHRR values obtained by mass loss cone [13] and MCC experiments and the corresponding percentage of physical and chemical mechanism occurring during burning.

Table 1 shows that both chemical and mechanical mechanisms occur during burning for the sol-gel treated PU foam.

Using TGA-FTIR on virgin PU and coated PU foams (Fig. 9), it is still possible to notice the characteristic peaks of the release of non-degraded DEP. Thus, the coating keeps its ability to act as a FR in both the condensed phase and the gas phase even in presence of PU foam.

These analyses also show that the coating starts to degrade before the PU foam. Indeed, Fig. 9 shows that ethanol starts to be released in

the gas phase at 220 °C (19 min) for the coated PU foam, but no peak characteristic of PU foam degradation is noticeable with or without the coating. Therefore, the intumescent process starts before the degradation of the PU foam, which explains the good protection of the underlying PU foam by the coating observed during UL94 and mass loss cone tests. Then, at around 390 °C (38 min), during the second swelling step, the characteristic peaks of ammonia, propylene and DEP are noticeable between the degradation peaks of the PU foam. The degradation products of the PU foam might also contribute to the swelling of the coating during this second step.

Py-GCMS analyses were thus carried out to see if the gases released by the PU foam contribute to the creation of the residue or if the gases released remain unchanged. Fig. 10 compares the Py-GCMS spectra of virgin and coated PU foams. It can be noticed that two peaks characteristic of the PU degradation (around 99 min) completely disappear when the PU foam is coated. These peaks correspond to isocyanate units obtained by depolymerization processes [16]. It can be concluded that the coating contributes in a positive manner to flame retard the PU foam by limiting its gas release during burning. These positive results motivated smoke release measurements.

Smoke box experiments allowed the measurement of CO₂ and CO release rate during burning. Tests were carried out on virgin PU foam and treated PU foam, the results are collected in Table 2.

It is clear that when the PU foam is treated with the sol-gel coating the gases released under the smoke box conditions are globally reduced (20% at 4min and 10% at 8 min for the CO₂ and 35% at 4 and 8 min for the CO). Thus, the coating protects the PU foam from burning but also decreases the global release of gases.

- Mechanism of action

Thanks to all the chemical analyses of the condensed and gas phases, a FR mechanism of action can be built (Fig. 11).

Around 190 °C, the first expansion step observed by rheological test is due to the release of ethanol (Py GC-MS, TGA-FTIR). It produces a white and fragile foamy residue. Then, around 380 °C, during the second expansion phase, three different gases are released by the coating, i.e. ammonia, propene and non-degraded DEP. A black and strong char is obtained. As proven by solid-state NMR, this char is composed of a Si-O-Si network mixed with phosphoric acid and silicophosphate. Thus, in the presence of a heating source, one part of DEP is released in the gas phase and contributes to the flame out, and another part turns into phosphoric acid (charring agent) in the intumescent system while APTES plays the role of a swelling agent, releasing ammonia in particular. The intumescent char obtained, composed of a foamed glassy layer of Si-O-Si, silicophosphate (Si-O-P) and phosphoric acid, stops the decomposition process (pyrolysis) and prevents the release of flammable gases, essentially cutting off fuel to the flame [33]. Thus, the flame retardant mechanism occurs in the condensed phase for the most part through an intumescent

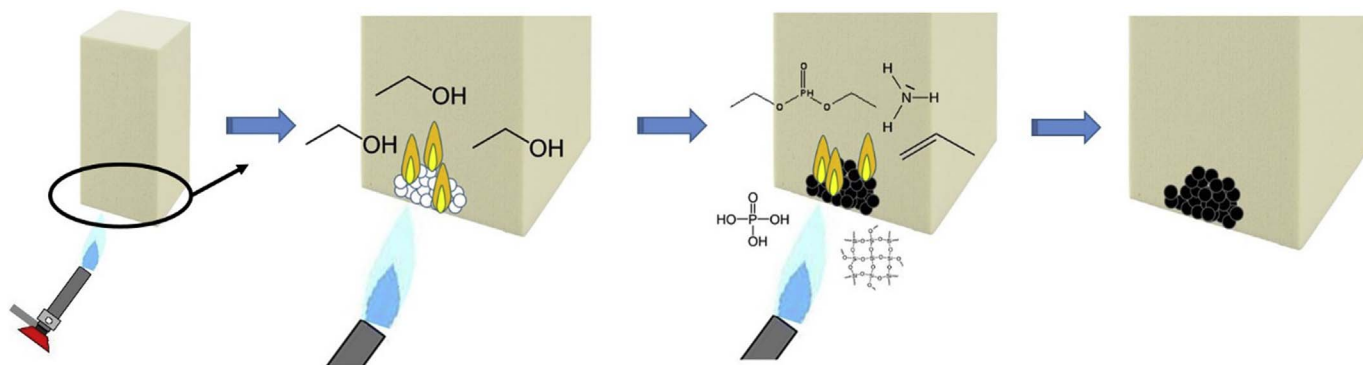


Fig. 11. Schema of the mechanism of action of the Sol/4APTES/2DEP FR coating when a flame is applied.

phenomenon. However, as revealed by Py-GCMS and TGA-FTIR analyses, a large quantity of non-degraded DEP and ammonia passes in the gas phase, which can participate in the flame retardant effect in the gas phase through chemical mechanisms (radical scavenger mechanisms, dilution effect, modification of the degradation path) and explain the significant decrease of HRR peak during the MCC test.

4. Conclusion

A sol-gel coating containing APTES and DEP was previously reported as an effective flame retardant for PU foam. The mechanism was studied by carrying out solid state NMR, rheometry, Py-GCMS, PCFC, TGA-FTIR and smoke box test. Solid state NMR showed that the residue was mainly a Si-O-Si and Si-O-P network mixed with phosphoric acid. An intrinsic intumescent phenomenon of the sol-gel coating was evidenced by rheological tests. Py-GCMS shows the release of ethanol, propene, ammonia and non-degraded DEP, which was confirmed by TGA-FTIR. The mechanism of action was determined to be a combination of a condense phase and a chemical mechanism. Indeed, the degradation of the coating gives all the ingredients for the intumescent phenomenon to occur, phosphoric acid (charring agent), ammonia (swelling agent) and DEP (acid source). When the coating is applied on PU foam, it builds a strong residue that slows down and even prevents the gas of degradation from being released in the gas phase, which protects the underlying PU foam from the flame. DEP and ammonia are released in the gas phase and can also act as a flame suppressant through chemical mechanisms (radical scavengers, dilution, modification of the degradation pathways). The coating is flame retardant by itself and does not require the PU foam substrate to be intumescent. Thus, this coating can potentially be applied on any substrate.

References

- [1] S.D. Shaw, A. Blum, R. Weber, K. Kannan, D. Rich, D. Lucas, C.P. Koshland, D. Dobraca, S. Hanson, L.S. Birnbaum, *Rev. Environ. Health* 25 (4) (2010) 261–305.
- [2] V. Babrauskas, A. Blum, R. Daley, L. Birnbaum, *Fire Saf. Sci.* (2011) 265–278.
- [3] J.O. Babayemi, O. Osibanjo, O. Sindiku, et al., *Environ. Sci. Pollut. Res.* (2016) 1–14.
- [4] Risk Assessment Report on Tris(2-chlor-propyl) Phosphate (TCPP), Scientific Committee on Health and Environmental Risks, Environmental Part, EINECS No. 237-158-7, 2007.
- [5] A. König, A. Malek, U. Fehrenbacher, G. Brunklaus, M. Wilhelm, T. Hirth, J. Cell. *Plastics* 46 (2010) 395–413.
- [6] J. Jang, H. Chung, M. Kim, H. Sung, *Polym. Test.* 19 (2000) 269–279.
- [7] M. Demirel, V. Pamuk, N. Dilsiz, J. Appl. *Polym. Sci.* 115 (2010) 2550–2555.
- [8] Y.S. Kim, R. Harris, R. Davis, *ACS Macro Lett.* 1 (2012) 820–824.
- [9] Y.C. Li, Y.S. Kim, J. Shields, R. Davis, *J. Mat. Chem. A* 1 (2013) 12987–12997.
- [10] K.M. Holder, M.E. Huff, M.N. Cosio, J.C. Grunlan, *J. Mat. Sci.* 50 (2015) 2451–2458.
- [11] F. Carosio, J. Alongi, *ACS Appl. Mat. Interfaces* 8 (10) (2016) 6315–6319.
- [12] M. Jimenez, N. Lesaffre, S. Bellayer, R. Dupretz, M. Vandenbossche, S. Duquesne, S. Bourbigot, *RSC Adv.* 5 (2015) 63853.
- [13] S. Bellayer, M. Jimenez, S. Barrau, S. Bourbigot, *RSC Adv.* 6 (2016) 28543–28554.
- [14] G. Tricot, J. Trebosc, F. Pourpoint, R. Gauvin, L. Delevoye, *Annu. Rep. NMR Spectrosc.* 81 (2014) 145–185.
- [15] S. Duquesne, S. Magnet, C. Jama, R. Delobel, *Polym. Degrad. Stab.* 88 (1) (2005) 63–69.
- [16] S. Duquesne, R. Delobel, M. Le Bras, G. Camino, *Polym. Degrad. Stab.* 77 (2) (2002) 333–344.
- [17] M. Jimenez, S. Bellayer, S. Duquesne, S. Bourbigot, *Surf. Coatings Technol.* 205 (3) (2010) 745–758 25.
- [18] Q. Wu, K.K. Gleason, *Plasma Polym.* 8 (1) (2003) 31.
- [19] M. Coquelle, S. Duquesne, M. Casetta, J. Sun, X. Gu, S. Zhang, S. Bourbigot, *Polymers* 7 (2) (2015) 316–332.
- [20] A.D. Naik, G. Fontaine, F. Samyn, X. Delva, J. Louisy, S. Bellayer, Y. Bourgeois, S. Bourbigot, *Fire Saf. J.* 70 (2014) 46–60.
- [21] F. Samyn, S. Bourbigot, *Polym. Degrad. Stab.* 97 (2012) 2217e2230.
- [22] C. Coelho, T. Azais, C. Bonhomme, L. Bonhomme-Coury, C. Boissière, G. Laurent, D. Massiot, *Comptes Rendus Chim.* 11 (2008) 387–397.
- [23] J. Alongi, G. Malucelli, *J. Mater. Chem.* 22 (41) (2012) 21805–21809.
- [24] B. Scharrel, *Materials* 3 (2010) 4710–4745.
- [25] F. Vilmin, I. Bottero, A. Travert, N. Malicki, F. Gaboriaud, A. Trivella, F. Thibault-Starzyk, *J. Phys. Chem. C* 118 (2014) 4056–4071.
- [26] S. Subianto, N.R. Choudhury, N.K. Dutta, *J. Polym. Sci. Part A Polym. Chem.* 46 (2008) 5431–5441.
- [27] P. Chevallier, A. Walter, A. Garofalo, I. Veksler, J. Lagueux, S. Begin-Colin, D. Felder-Flesch, M.-A. Fortin, *J. Mat. Chem. B* 2 (2014) 1779–1790.
- [28] Hadi Manap, Gerald Dooly, Sinead O’Keeffe, Elfed Lewis, *Sensors Actuators B Chem.* 154 (2) (20 June 2011) 226–231.
- [29] O.P. Korobeinichev, T.A. Bolshova, A.G. Shmakov, V.M. Shvartsberg, *Combust. Explos. Shock Waves* 50 (No. 2) (2014) 130–134.
- [30] A. Rangobin, G. Fontaine, C. Penverne, S. Bourbigot, *Materials* 10 (2017) 665.
- [31] R. Sonnier, L. Ferry, C. Longuet, F. Laoutid, B. Friederich, A. Laachachi, J.-M. Lopez-Cuesta, *Polym. Adv. Technol.* 22 (2011) 1091–1099.
- [32] B. Friederich, A. Laachachi, M. Ferriol, M. Cochez, R. Sonnier, V. Toniazzo, D. Ruch, *Polym. Degrad. Stab.* 97 (2012) 2154–2161.
- [33] J. Alongi, G. Malucelli, *J. Mater. Chem.* 22 (41) (2012) 21805–21809.